COMPUTATIONAL INVESTIGATION ON ELECTRONIC STRUCTURES AND PROPERTIES OF 4,6-BIS(NITROIMINO)-1,3,5-TRIAZINAN-2-ONE: AN INSENSITIVE MUNITIONS COMPOUND

by
Katarina Pittman

A thesis submitted to the faculty of The University of Mississippi in partial fulfillment of the requirements of the Sally McDonnell Barksdale Honors College.

Oxford
May 2018

Approved by

Advisor: Professor Gregory Tschumper

Reader: Professor Adam Smith

Reader: Professor Nathan Hammer

Dedication

To my family, in particular my late grandfather. I will always love you.

Acknowledgements

This work was supported in part by a grant of computer time from the DOD High Performance Computing Modernization Program at ERDC, Vicksburg.

Additionally, I would like to thank my advisor, Dr. Tschumper, for his patience and encouragement; the Ole Miss Chemical Engineering Department, for believing in me even when I didn't believe in myself; my friends, for motivating me and making me smile even during the stressful times; and the Sally McDonnell Barksdale Honors College, for providing a memorable educational experience.

Contents

ABSTRACT

In order to minimize unintentional detonation, current munitions research has focused on the development of chemical compounds that are insensitive to external stimuli whilst maintaining their effectiveness. While these compounds, known as high performance insensitive munitions compounds, are promising in terms of potency and stability, their environmental impacts have either not been fully understood or are yet to be investigated. In the present research, we have performed a computational chemistry investigation on electronic structures and properties of an insensitive munition compound 4,6-bis(nitroimino)-1,3,5-triazinan-2-one (DNAM). The Density Functional Theory using the B3LYP and M06-2X functionals and MP2 methodology were used for geometry optimization of various tautomeric forms of DNAM. The effect of bulk water solution was evaluated using the conductor-polarizable calculation model (CPCM) and the SMD solvation model. Ionization potential, electron affinity, redox properties, and pKa values were also computed and were compared with the available experimental data. It was revealed that DNAM can exist in different tautomeric forms. Different physical and chemical properties of DNAM will be discussed.

1 Introduction

1.1 Computational Chemistry

Computational chemistry is a branch of chemistry that uses computers in order to investigate chemical problems by understanding the behavior of atoms and molecules. It allows the chemist to solve for such properties as molecular geometries, which give the shape of molecules; energies of molecules and their transition states, which can demonstrate how fast a reaction can occur and which isomer is favored at equilibrium; spectra, including UV and IR; and more. In order to understand these properties, the computational chemist uses many different tools, including molecular dynamics, *ab initio*, semi empirical calculations, density functional theory (DFT), and molecular dynamics calculations.

When imagining a system of a well-defined collection of atoms, it is important to understand the energy of these atoms and how they change as the atoms move. However, before we are able to tackle this problem, the computational chemist needs to define the location of the nucleus of an atom and its electrons. This is enabled via the Schrödinger equation, a fundamental equation in modern physics. Based on quantum mechanics, *ab initio* (Latin for "from the beginning") calculations use the Schrödinger equation, although it cannot be solved exactly in one-electron systems and must therefore use approximations. DFT, also based on the Schrödinger equation, derives the electron distribution rather than calculating a wave function as in *ab initio*, yielding an approximate solution.

In comparison to experiment, computational chemistry demonstrates several advantages in that it is cheaper, quicker, and environmentally safe. Although it does not replace

the importance of experiment, it is an important aspect of chemistry rooted in the philosophy that chemistry is best understood through the behavior of atoms and molecules.[1]

1.2 The Schrödinger Equation

In the late nineteenth century, the physics community encountered a puzzle: blackbody radiation. This is when an object, known as a blackbody, perfectly absorbs all radiation without reflection. Classical physics had predicted that the flux density (the change in flux per wavelength emitted by a wavelength range) should approach zero. A solution was finally given when Max Planck produced the equation

$$E = h\nu = \hbar\omega \tag{1}$$

which suggested that light with a certain frequency ν is emitted in quantized lumps of energy and where h, known as Planck's constant, is approximately 6.63×10^{-34} J·s, with $\hbar$ being equal to $\frac{h}{2\pi}$ and ω equal to $2\pi\nu$. By hypothesizing quantized radiation, the problem of infinity was solved. In 1905, Albert Einstein found that such quantization was inherent in light, which he dubbed the photoelectric effect. Since $E = pc$ for any massless particle, which includes photons, and $\omega = ck$ for a light wave, Equation 1 becomes:

$$pc = \hbar(ck) \tag{2}$$

$$p = \hbar k \tag{3}$$

relating the momentum of a photon (p) to the wavenumber of the wave with which it is associated.

By 1913, Niels Bohr stated that electrons exhibit wavelike properties, and only a few

years later, Louis de Broglie proposed that all particles were associated with waves, even massive ones. This proposal led to the problem of wave-particle duality: sometimes things can exhibit the behavior of a wave, and sometimes things behave like particles.

In order to understand how waves evolve in space and time, Edwin Schrödinger in 1926 formulated a wave equation known as the Schrödinger equation. However, the correct interpretation of the wave was not understood by Schrödinger himself, but by Max Born, who found that the wave is a probability amplitude. By squaring the absolute value of a wave, one can obtain the probability of finding a particle at a given location, provided that it is a function of x.[2]

To rationalize the development of the Schrödinger equation, one begins by writing the expression for a standing wave, where the amplitude of the wave, represented by $f(x)$ or ψ, varies with time and with a distance x from end-to-end:

$$\frac{d^2\psi}{dx^2} = \frac{-4\pi^2}{\lambda^2}\psi \tag{4}$$

where λ is the wavelength, equal to $\frac{h}{mv}$, where m is the mass of the particle and v is the velocity. Substituting this expression for λ:

$$\frac{d^2\psi}{dx^2} = \frac{-4\pi^2 m^2 v^2}{h^2}\psi \tag{5}$$

Noting that the energy of a particle (E) is simply the sum of its kinetic and potential energies (V), and recognizing that kinetic energy is equal to $\frac{1}{2}mv^2$, we are able to finally find the Schrödinger equation in one dimension:

$$\frac{d^2\psi}{dx^2} = \frac{-8\pi^2 m}{h^2}(E-V)\psi \tag{6}$$

In order to bring this equation into the third dimension, one replaces $\frac{d^2}{dx^2}$ with $\frac{d^2}{dx^2} + \frac{d^2}{dy^2} + \frac{d^2}{dz^2}$, simply represented by the Laplacian operator ∇^2:

$$\nabla^2\psi + \frac{8\pi^2 m}{h^2}(E - V)\psi = 0 \tag{7}$$

$$(\frac{h^2}{8\pi^2 m}\nabla^2 + V)\psi = E\psi \tag{8}$$

$$\hat{H}\psi = E\psi \tag{9}$$

$\hat{H}$ is an operator known as the Hamiltonian operator, specifying that an operation is to be performed on ψ, and the result of that operation is equal to E multiplied by ψ; in short, $\hat{H}\psi$ does not mean $\hat{H}$ times ψ, but rather $\hat{H}$ of ψ. E, being a constant, is the eigenvalue, whereas ψ is an eigenfunction.[1]

However, this equation can only successfully be solved in systems with one electron, such as the hydrogen atom. To be able to solve the Schrödinger equation for a multi-electron system, the wave function needs to be approximated with fewer variables, which is when the Born-Oppenheimer approximation is utilized. Since the electrons have a mass that is significantly smaller than that of the nucleus, one can assume that the nuclei are essentially stationary in comparison to the electrons, and therefore electronic and nuclear motion can be separated. The part dependent on the position of the nuclei is associated with the vibration of the molecule, while the other is dependent on the positions of the electrons at a fixed position of all the nuclei.[3] Despite these assumptions, the Schrödinger equation is still a challenge to solve, and this is how computational programs prove to be especially useful.

1.3 Insensitive Munitions Compounds

An explosive is defined as a substance that, upon undergoing a chemical reaction, releases a significant amount of heat and exerts high pressure on surroundings. Such a chemical

reaction is stimulated when the compound or compounds are subjected to friction, impact, spark, or shock and undergo rapid decomposition through the transference of chemical energy on the molecular level to macroscopic kinetic energy. Useful in situations where high rates of energy application and high pressures are needed, explosives have both industrial and military applications, the latter applying in particular to the U.S. Department of Defense (DOD).[4]

Explosives can be divided into two categories: primary and secondary. Primary explosives, in comparison to secondary, exhibit lower detonation pressures and velocities and heat of detonation. In addition to less power than its counterpart, primary explosives also require extreme care in handling, as they are able to quickly reach detonation. Conversely, secondary explosives are significantly less sensitive to electrostatic discharge, heat, friction, and impact; in fact, it is often used in conjunction with a primary explosive, with the impact from the primary explosive initiating detonation of the more powerful secondary explosive. However, with the increased demand for a higher performing explosive with lower sensitivity to impact, friction, electrostatic discharge, heat, and shock, combined with environmental and toxicological concerns regarding the lead content in primary explosives, secondary explosives are prime candidates for munitions research.[5]

Primarily used as secondary explosives, high-energy density materials (HEDMs) store and release energy through making and breaking bonds. Their fundamental properties include oxygen balance, density, heat of formation, sensitivity, thermal and hydrolytic stability, and environmental acceptability. They derive most of their energy from either oxidation of the carbon backbone, which is seen in classic munitions such as trinitrotoluene (TNT) and 1,3,5-trinitro-1,3,5-triazinane (RDX); or very high positive heats of formation, as seen in compounds containing a considerable amount of nitrogen.[6]

In the past, the former category was widely considered as best for weapon applications. However, with several incidents of unintentional detonation due to impact or shock in such situations as aircraft carriers and munitions trains have made these munitions less attractive

to the DOD. The development of munitions with higher thermal stability and low sensitivity to impact has become critical. The motive for decrease in susceptibility has given the secondary explosive-based formulations the title ”insensitive munitions.” In addition to minimizing unintended detonation of nearby explosives, they exhibit fulfillment of the criteria for which current munitions research has been actively searching: low toxicity and natural degradation pathways and products.[5]

Rather than deriving energy from overall heats of combustion, high energy density materials exhibits a significant number of N-N and C-N bonds, which are inherently energetic in that they exhibit large positive heats of formation. In particular, bicyclic heterocycles give excellent combinations of stability, oxygen balance, and density in addition to these higher heats of formation, with energetic salts that are considered more acceptable for the environment due to the high percentage of dinitrogen in decomposition products. The lower percentage of carbon and hydrogen have several positive effects, including an acceptable oxygen balance, an enhancement in density, and a large number of moles of gas product per gram HEDM.[4]

Additionally, the presence of adjacent nitrogen atoms in these compounds are positioned to form nitrogen gas upon detonation. Nitrogen is unique in that the bond energy per two-electron bond increases from a single bond to a double bond to a triple bond, demonstrating that dinitrogen is the most stable of polynitrogen species. This is promising in terms of creating highly energetic materials that are also environmentally friendly.[4]

Current research has been pursuant of the development of accurate models and simulations of energetic materials. Additionally, the concern for environmental hazards associated with their use has called for predictive data concerning the environmental impact of a material before consideration for use. Quantum mechanical methods have been used on a broad range of high-nitrogen containing materials, including stability rankings among possible conformers and vibrational spectra. Theoretical studies are undoubtedly instrumental in the development of insensitive munitions.[6]

1.4 4,6-bis(nitroimino)-1,3,5-triazinan-2-one (DNAM)

While legacy high energy density materials such as 2,4,6-trinitrotoluene (TNT) serve as effective munitions compounds, they can have a relatively high risk of unintentional detonation during manufacture or transport due to their sensitivity to external stimuli. Consequently, there is an increased interest in the development of high energy density materials that are not only insensitive to external stimuli, but also maintain effectiveness while minimizing their environmental impact. These materials, dubbed insensitive munitions, demonstrate high thermal stability and low impact sensitivity to friction and electrostatic discharge.[7]

Certain heterocyclic nitrogen-containing compounds form highly energetic salts that are both effective munitions candidates yet environmentally safe due to the high percentage of dinitrogen in their decomposition products. Furthermore, they have the advantage of high positive heats of formation rather than heats of combustion as in the case of traditional munitions. One promising material is 4,6-bis(nitroimino)-1,3,5-triazinan-2-one (also known as 4,6-dinitramino-1,3,5-triazine-2(1H)-one, dinitroammeline, or simply DNAM). First synthesized in 1951,[8] this compound has been shown to exhibit the aforementioned characteristics desired in insensitive munitions.

Although DNAM has been the subject of several theoretical studies, a limited number of efforts have focused specifically on the most stable conformers. Only recently have the tautomers of the compound been characterized theoretically, when Simões et al. conducted a joint theoretical and experimental investigation on DNAM using MP2 and density functional theory (DFT) methods in 2007. They found that gas phase tautomers possessing nitroimine groups are more stable than those with nitramine groups. Of these tautomers, the so-called NIC (nitro, imine, keto) series was identified as the most probable nitroimine forms, with its third conformer found to exist in crystal form. The following year, Gao et al. examined the thermal stabilities of several energetic salts using the Born-Haber energy cycle to determine heats of formation. In addition to the triazole salts being thermally

stable, the detonation velocities and pressures were comparable to those of common explosives, exceeding those of TNT.[7] DNAM salts also exhibited large positive heats of formation. Little investigation has been conducted regarding the acidity of DNAM; in 2001, the Henderson-Hasselbalch equation was utilized to confirm the acidic nature of the compound, and further investigation as to the decomposition pathway of DNAM in aqueous solution was encouraged.[9]

In this work, we build on the significant contributions of these prior efforts by examining the effects of water solvation on DNAM with bulk water using implicit solvation models. Through relative energies, vertical/adiabatic electron affinities and ionization potentials, and reduction/oxidation (redox) potentials, this paper highlights the differences between the three conformers and examines the manner in which DNAM responds to an aqueous environment by exploring potential reactivity. The ionization pK_a's are also computed for future determination of the degree of ionization and propensity for sorption to soil and sediment, which is highly significant in determining environmental fate. This in turn allows consideration of DNAM's reaction kinetics, complexation, and more.

2 Methods

2.1 Computational Methods

In this study, we optimized geometries using two quantum chemical methods based on density functional theory (DFT) as well as second-order Møller-Plesset perturbation theory (MP2),[10–13] all in conjunction with the Pople-style split valence basis set 6-311++G(d,p). We utilized both Becke-style 3-parameter exchange functional combined with the Lee-Yang-Parr correlation functional (B3LYP) and Minnesota 06 hybrid functional (M06-2X) as implemented in Gaussian16 for comparison.[14] Harmonic vibrational frequencies were calculated in the harmonic approximation using the same methods and basis set. The absence of imaginary frequencies confirms that the three conformers are at a minimum on their respective potential energy surfaces. In order to consider structural changes in solution, geometry optimizations and corresponding harmonic vibrational frequency calculations were additionally performed using continuum solvation models (CPCM[15] and SMD[16]) with the default solvent parameters for water available in Gaussian16.

2.2 Conformers

In previous studies concerning DNAM, four tautomeric forms have been identified — NAC, NAE, NIC, and NIE (with the NIC series identified as the most stable tautomer by more than 20 kcal mol^{-1}[17]) . The tautomers are distinguished by the presence of keto versus enol ("C" vs "E") and nitroimine versus nitramine ("NI" vs "NA") moieties, as can be seen in Figure 1 where examples of each tautomer are depicted.

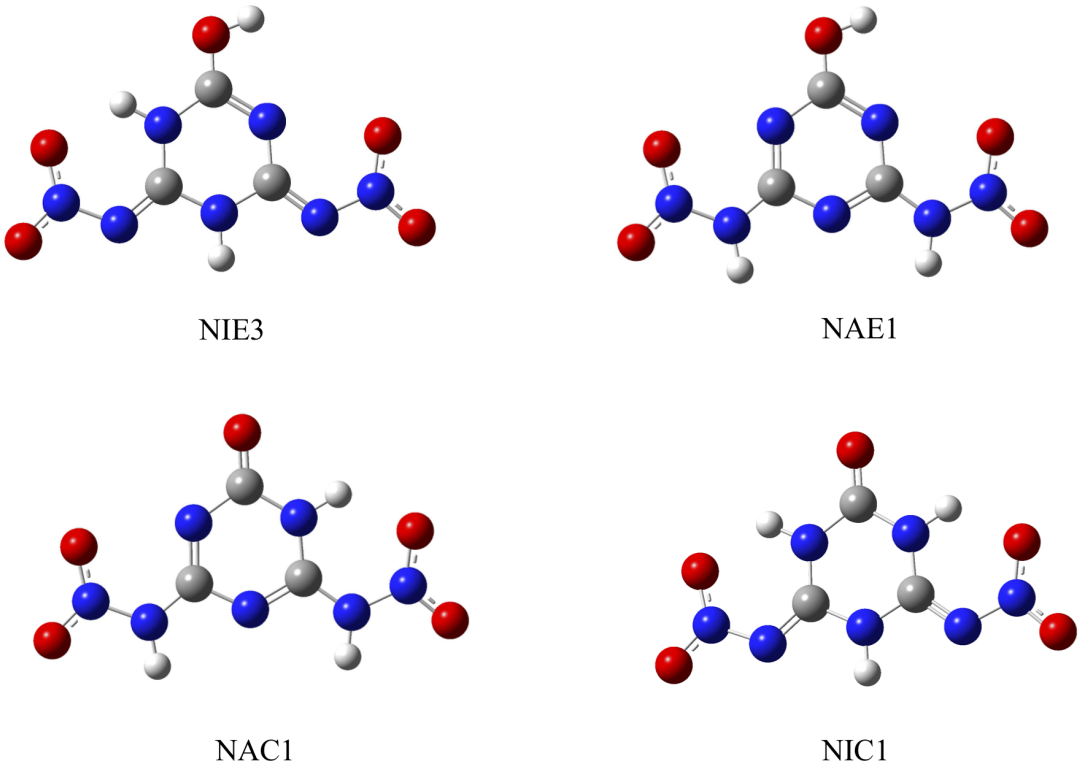

Figure 1: One conformer from each of the four tautomer groups (NAC, NAE, NIC, and NIE).

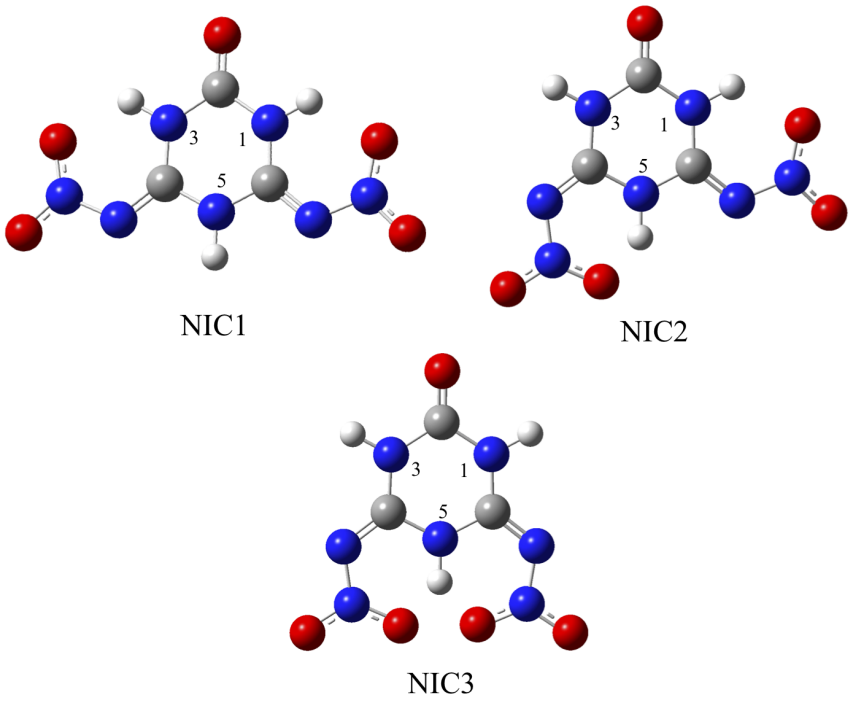

Figure 2: One conformer from each of the four tautomer groups (NAC, NAE, NIC, and NIE).

In this study, we focused on the NIC series, which possesses the keto and nitroimine moieties and has three conformers determined by the orientation of the nitro groups (i.e., NIC1, NIC2, and NIC3), which are displayed in Figure 2.

2.3 Thermochemistry

Adiabatic electron affinities (EA) and ionization potentials (IP) were calculated by taking the difference between the total energy of the fully optimized neutral ground state of DNAM $E^{\text{opt}}_{\text{neutral}}$ and that of its fully optimized negative (anion) or positive (cation) radical ion ($E^{\text{opt}}_{\text{anion}}$ and $E^{\text{opt}}_{\text{cation}}$, respectively), as shown in Equations 10 and 11.

$$\mathrm{AEA} = -(E^{\mathrm{opt}}_{\mathrm{anion}} - E^{\mathrm{opt}}_{\mathrm{neutral}}) \tag{10}$$

$$\mathrm{AIP} = \quad E^{\mathrm{opt}}_{\mathrm{cation}} - E^{\mathrm{opt}}_{\mathrm{neutral}} \tag{11}$$

For the vertical values, the ion radicals are computed for the corresponding one-electron reduced or oxidized forms at the corresponding neutral optimized geometry ($E^{\mathrm{neutral}}_{\mathrm{anion}}$ and $E^{\mathrm{neutral}}_{\mathrm{cation}}$, respectively).[18]

$$\mathrm{VEA} = -(E^{\mathrm{neutral}}_{\mathrm{anion}} - E^{\mathrm{opt}}_{\mathrm{neutral}}) \tag{12}$$

$$\mathrm{VIP} = \quad E^{\mathrm{neutral}}_{\mathrm{cation}} - E^{\mathrm{opt}}_{\mathrm{neutral}} \tag{13}$$

For the reduction potentials in both the gas phase and in solution, we employed the Nernst equation,

$$E^{\circ}_{\mathrm{red}} = -\frac{\Delta G^{\circ}_{\mathrm{red}}}{nF} + E_{\mathrm{H}} \tag{14}$$

$$E^{\circ}_{\mathrm{ox}} = \frac{\Delta G^{\circ}_{\mathrm{ox}}}{nF} + E_{\mathrm{H}} \tag{15}$$

where E°_{red} and E°_{ox} are the reduction and oxidation potentials, respectively, in either the gas phase or in solution; n is the number of electrons (n=1); F is the Faraday constant (96,485 C mol^{-1}); and E_{H} is the potential for the standard hydrogen electrode (4.4 V). $\Delta G^{\circ}_{\mathrm{red}}$ is the Gibbs free energy required to attach an electron to the DNAM conformer in either the gas phase or in solution, and likewise $\Delta G^{\circ}_{\mathrm{ox}}$ is the Gibbs free energy necessary to remove an electron in the gas phase or in solution. These terms may be interpreted as simple differences in Gibbs energy between the radical and neutral species, as shown for

the gas phase quanties in Equations 16 and 17.

$$\Delta G^{\circ}_{\text{red,gas}} = G^{\text{opt}}_{\text{anion,gas}} - G^{\text{opt}}_{\text{neutral,gas}} \tag{16}$$

$$\Delta G^{\circ}_{\text{ox,gas}} = G^{\text{opt}}_{\text{cation,gas}} - G^{\text{opt}}_{\text{neutral,gas}} \tag{17}$$

The bulk solution phase equations are often written in terms of the $\Delta G^{\circ}_{\text{gas}}$ adjusted by the change in Gibbs energy due to solvation of each species involved, as can be seen in Equations 18 and 19

$$\Delta G^{\circ}_{\text{red,solv}} = \Delta G^{\circ}_{\text{red,gas}} + \Delta\Delta G^{\circ}_{\text{red,solv}} \tag{18}$$

$$\Delta G^{\circ}_{\text{ox,solv}} = \Delta G^{\circ}_{\text{ox,gas}} + \Delta\Delta G^{\circ}_{\text{ox,solv}} \tag{19}$$

where the $\Delta\Delta G^{o}$ quantities are defined as

$$\Delta\Delta G^{\circ}_{\text{red,solv}} = \Delta G^{\circ}_{\text{anion,solv}} - \Delta G^{\circ}_{\text{neutral,solv}} \tag{20}$$

$$= G^{\text{opt}}_{\text{anion,solv}} - G^{\text{opt}}_{\text{anion,gas}} - [G^{\text{opt}}_{\text{neutral,solv}} - G^{\text{opt}}_{\text{neutral,gas}}] \tag{21}$$

with an analogous expression for $\Delta\Delta G^{\circ}_{\text{ox,solv}}$.

In calculating the pK_as, we considered the single deprotonation of DNAM. The resulting anionic form of DNAM was accomplished by deprotonating one of the three nitrogens in the central triazine ring. NIC1 and NIC3 were only deprotonated at two nitrogens (N1 and N5), due to the symmetric nature of the nitro groups, while all three nitrogens in NIC2 were deprotonated (N1, N3, and N5). The labeling of the ring nitrogens are shown in 2. For the pK_a calculations, we used the following equation,

$$\text{pK}_\text{a} = \frac{\Delta G_{\text{solv}}}{RT\ln 10} \tag{22}$$

where R is the gas constant in kcal mol^{-1} K^{-1} and T is the temperature of the system

(298.15 K). The ΔG_{solv} may be solved in a similar manner to Equations 18 and 19, but the species involved are the acidic form of DNAM, the conjugate base and the hydrogen ion as shown below:

$$\Delta G_{\text{solv}} = \Delta G_{\text{gas}} + \Delta\Delta G_{\text{solv}} \tag{23}$$

where ΔG_{gas} is expressed as,

$$\Delta G_{\text{gas}} = G_{\text{gas}}(\text{H}^+) + G_{\text{gas}}(\text{DNAM}^-) - G_{\text{gas}}(\text{DNAM}) \tag{24}$$

and $\Delta\Delta G_{\text{solv}}$ is,

$$\Delta\Delta G_{\text{solv}} = \Delta G_{\text{solv}}(\text{H}^+) + \Delta G_{\text{solv}}(\text{DNAM}^-) - \Delta G_{\text{solv}}(\text{DNAM}). \tag{25}$$

The terms involving H^+ present a challenge and can give rise to large errors in pK_a calculations. Thus we have chosen to apply an experimental determination of $\Delta G_{\text{solv}}(H^+)$, using the value of -265.9 kcal mol^{-1} as recommended by Alongi and Shields, while $G_{\text{gas}}(\text{H}^+)$ has been determined experimentally and is widely accepted as -6.28 kcal mol^{-1} at 1 atm.[19] In addition, calculations require the conversion of standard state from 1 mol atm^{-1} to 1 mol L^{-1}, notated as $\Delta G^{\circ\rightarrow *}$. The correction cancels for all but one term and we arrive at the correction factor as follows:

$$\Delta G^{\circ\rightarrow *} = RT\ln(24.4564) \tag{26}$$

yielding 1.89 kcal mol^{-1} at a temperature of 298.15 K.

As a comparison for pK_a calculations, we also used COSMOTherm, a software specializing in predictive property calculations of liquids (data may be found in Supplementary-Information).

3 Results and Discussion

Table 1 displays the relative electronic energies with and without solvation models. In the gas phase, the NIC1 and NIC2 conformers are approximately isoenergetic and lowest in energy across all three methods used, which is consistent with previous theoretical studies.[17] The trends in the CPCM and SMD solvation models mirror those in the gas phase; however, the relative energies with implicit solvent tend to decrease relative to the gas phase, especially for the NIC3 conformer. For example, the B3LYP energy for the NIC3 conformer is 1.76 kJ mol^{-1} in the gas phase, but decreases to 0.67 kJ mol^{-1} and 0.58 kJ mol^{-1} for CPCM and SMD, respectively. Differences between DFT functionals and MP2 are small, but the greatest differences arise for the NIC3 conformer again. In the gas phase, the MP2 relative energy for NIC3 is 0.9 kJ mol^{-1} compared to 1.76 and 1.24 kJ mol^{-1} for BLYP and M06-2X, respectively.

Table 1: Relative electronic energies (ΔE in kJ mol^{-1}) using B3LYP, M06-2X, and MP2 levels and the 6-311++G(d,p) basis set.

Solvation Model	Conformer	B3LYP	M06-2X	MP2
None	NIC1	0.00	0.00	0.00
	NIC2	0.07	0.17	0.13
	NIC3	1.76	1.24	0.90
CPCM	NIC1	0.00	0.00	0.00
	NIC2	0.08	0.15	0.09
	NIC3	0.67	0.25	0.27
SMD	NIC1	0.00	0.00	0.01
	NIC2	0.01	0.06	0.00
	NIC3	0.58	0.20	0.13

Calculation of EA's and IP's, displayed in Table 2, reveal similar trends in the gas

phase and bulk solution results. All methods are in fair agreement - MP2 typically yields the lowest magnitude values for EA and IP, with M06-2X usually falling in between MP2 and B3LYP. Variations (increases or decreases) tend to be largest for DFT methods used with the SMD model, for both vertical and adiabatic values. When comparing EA's in the gas phase versus that of the solvation models, NIC1 and NIC2 consistently demonstrate the smallest change (averaging 1.47 eV when using CPCM and 1.58 with SMD), whereas when using the NIC3 conformer this difference grows, averaging 1.64 eV using CPCM and 1.68 eV with SMD. However, this trend is reversed in the case of IP's; NIC1 and NIC2 demonstrate the greatest difference when compared to the gas phase (average of 2.13 eV and 2.37 eV for CPCM and SMD, respectively), while NIC3 averages 1.84 eV with CPCM and 2.1 eV with SMD. These trends also demonstrate that there is a significant increase in EA when solvation models are applied, while IP's lower considerably. This suggests that in water, DNAM undergoes an increase in reactivity.

This increase in reactivity with the inclusion of bulk solvation effects is also manifested in the reduction potentials, compiled in Table 3. The use of solvation models demonstrates a notable increase in reduction potentials (i.e., less negative), while the oxidation potentials are shifted to lower values (i.e., less positive). These differences are most prominent when using the SMD solvation model. The reduction potentials shift less with the M06-2X functional compared to B3LYP and also demonstrate a greater difference when comparing the use of solvation models with the gas phase. Regardless of the method used, NIC2 and NIC3 both display similar reduction potentials when using solvation models, whereas in the gas phase NIC1 and NIC3 are more similar. Nonetheless, all reduction potentials are negative, which suggests that DNAM remains resistant to reduction in bulk water.

The oxidation potentials decrease with the inclusion of solvent effects but remain positive. While the DFT results clearly change (by 2-3 eV for a given conformer) when CPCM or SMD are applied, the MP2 data remain consistent in gas phase and in bulk solution, differing by approximately 0.2 eV. Additionally, MP2 predicts NIC2 and NIC3 oxidation

Table 2: Vertical and adiabatic electron affinities (EA) and ionization potentials (IP) in eV computed using B3LYP, M06-2X, and MP2 with the 6-311++G(d,p) basis set.

Vertical							
Solvation Model	Conformer	B3LYP		M06-2X		MP2	
		EA	IP	EA	IP	EA	IP
None	NIC1	2.09	10.38	1.78	10.99	1.02	11.31
	NIC2	2.12	10.37	1.83	11.05	1.01	11.50
	NIC3	2.02	10.31	1.74	11.35	0.97	11.00
CPCM	NIC1	3.63	8.27	3.12	8.99	2.42	9.01
	NIC2	3.66	8.34	3.05	9.01	2.50	9.18
	NIC3	3.68	8.74	3.43	9.17	2.62	8.64
SMD	NIC1	3.70	8.08	3.24	8.71	2.17	8.72
	NIC2	3.74	8.12	3.28	8.78	2.35	8.81
	NIC3	3.76	8.46	3.31	8.90	2.56	8.34

Adiabatic							
Solvation Model	Conformer	B3LYP		M06-2X		MP2	
		EA	IP	EA	IP	EA	IP
None	NIC1	2.35	10.14	2.09	10.64	1.23	10.29
	NIC2	2.39	10.21	2.15	10.62	1.26	10.29
	NIC3	2.32	10.10	2.11	10.55	1.27	10.26
CPCM	NIC1	3.84	8.00	3.67	8.35	2.60	7.99
	NIC2	3.88	8.02	3.71	8.35	2.79	8.04
	NIC3	3.89	8.00	3.74	9.03	2.79	8.03
SMD	NIC1	3.88	7.73	3.80	8.09	2.59	7.69
	NIC2	3.93	7.78	3.85	8.13	2.66	7.73
	NIC3	3.97	7.75	3.87	8.76	3.72	7.74

potentials to be roughly 2.0 eV smaller in magnitude than NIC1, whereas all three conformers yield similar results in each phase for DFT. In each DFT functional used, there is a markedly smaller difference in oxidation potentials in the NIC3 conformer when comparing the gas phase and solvation models, displaying only a 1.84 eV difference while the other conformers average a 2.51 eV difference with the SMD model. However, it is still apparent that the oxidation potential of every conformer decreases when in a bulk water environment for DFT predictions, while MP2 is relatively consistent in all phases.

Table 3: Reduction (Red) and oxidation (Ox) potentials using B3LYP and M06-2X with the 6-311++G(d,p) basis set. All values are shown in eV.

Solvation Model	Conformer	B3LYP		M06-2X		MP2	
		Red	Ox	Red	Ox	Red	Ox
None	NIC1	-2.02	5.77	-2.24	6.25	-3.19	5.77
	NIC2	-1.97	5.82	-2.19	6.23	-3.21	5.76
	NIC3	-2.02	5.70	-2.23	6.16	-3.37	5.80
CPCM	NIC1	-0.54	3.63	-0.66	3.97	-1.75	3.54
	NIC2	-0.43	3.65	-0.60	3.94	-1.48	3.57
	NIC3	-0.47	3.65	-0.59	4.69	-1.63	3.55
SMD	NIC1	-0.49	3.39	-0.53	3.71	-1.96	3.23
	NIC2	-0.39	3.42	-0.48	3.75	-2.16	3.28
	NIC3	-0.34	3.40	-0.46	4.32	-1.69	3.31

As can be seen from the structures of the NIC series (Figure 2), the nitroimino functional groups provide an electron-withdrawing effect, lending little basic character to the species. This is apparent in the pK_a results shown in Table 4, where the majority of pK_a values range from around -3 to 1 (relatively strong acid to weak acid). M06-2X tends to yield the most acidic pK_as; for example, the N5 nitrogen of NIC1/M06-2X/SMD has a pK_a of -5.29 compared to -1.92 for B3LYP/SMD. Nonetheless, the N5 nitrogen is generally the most acidic for all methods, with B3LYP/CPCM NIC3 and B3LYP/SMD for NIC3 being the notable exceptions; and the N1 site is predicted to be the most basic (with few exceptions: B3LYP for CPCM and SMD).

Table 4: Predicted pK_a values using B3LYP and M06-2X levels and the 6-311++G(d,p) basis set. All values are shown in kJ mol^{-1}.

Conformer	Nitrogen	CPCM		SMD	
		B3LYP	M06-2X	B3LYP	M06-2X
NIC1	N1	1.54	-1.69	1.49	-1.71
	N5	-2.78	-4.47	-1.92	-5.29
NIC2	N1	1.58	-1.19	1.29	-1.33
	N3	-0.09	-2.46	-0.33	-2.54
	N5	-0.87	-3.69	-1.11	-3.37
NIC3	N1	0.38	-1.52	-0.76	-2.26
	N5	0.61	-2.61	0.49	-2.51

4 Conclusions

In this study, we investigated the effect of the solvation models CPCM and SMD on the nitroimine ketone tautomers of DNAM through analysis of relative energies, electron affinities and ionization potentials, redox potentials, and pK_as using DFT (B3LYP, M06-2X functionals) and MP2. The M06-2X tended to fall between the B3LYP and MP2 values, and the MP2 data typically showed the least sensitivity to phase/solvation model. Our calculations predict that, in a bulk water environment, DNAM's electron affinities increase and ionization potentials decrease for each NIC conformer. This corresponds to the results from the redox potentials, with the reduction potentials becoming more positive and the oxidation potentials becoming less so with solvation models applied. However, DNAM continues to be resistant to reduction in a bulk water environment, since the reduction potentials remain negative. Shifts in results due to solvation model were most prominent when using the SMD solvation model. The pK_a calculations confirm the electron-withdrawing nature of the nitroimine groups, which lends an acidic character to the triazine ring. Overall, our results suggest no major changes in reactivity with only modest shifts in electronic properties of DNAM in bulk solution. Furthermore, DNAM is likely deprotonated at the N5 position at all but the most acidic pH's (less than 2). Further studies should include the effects of different species present in water that may influence the reactivity or degradation of DNAM when interacting with water.

References

[1] Errol G. Lewars. *Computational Chemistry: Introduction to the Theory and Applications of Molecular and Quantum Mechanics*. Springer, New York, 2011.

[2] David Morin. Introduction to quantum mechanics. Technical report, Harvard University, Cambridge, MA, 2010.

[3] David S. Sholl and Janice A. Steckel. *DENSITY FUNCTIONAL THEORY*. John Wiley & Sons, Inc., Hoboken, New Jersey, 2009.

[4] Haixiang Gao and Jeanne M. Shreeve. Azole-based energetic salts. *Chemical Reviews*, 111(11):7377–7436, 2011.

[5] Jesse Sabatini and Karl Oyler. Recent Advances in the Synthesis of High Explosive Materials. *Crystals*, 6(1):5, 2015.

[6] Thomas J. Meyer, Peter Day, Xue Duan, Jean-Pierre Sauvage, Gerard Parkin, and Herbert W Roesky. Structure and Bonding. *Structure and Bonding*, 76(7), 2014.

[7] Haixiang Gao, Yangen Huang, Chengfeng Ye, Brendan Twamley, and Jean'ne M. Shreeve. The synthesis of di(aminoguanidine) 5-nitroiminotetrazolate: Some diprotic or monoprotic acids as precursors of energetic salts. *Chemistry - A European Journal*, 14(18):5596–5603, 2008.

[8] Edward R. Atkinson. The Nitration of Melamine and of Triacetylmelamine. *Journal of the American Chemical Society*, 73(9):4443–4444, 1951.

[9] P. Simões, L. Pedroso, A. Portugal, I. Plaksin, and J. Campos. New propellant component, part II. Study of a PSAN/ DNAM/HTPB based formulation. *Propellants, Explosives, Pyrotechnics*, 26(6):278–283, 2001.

[10] Chr. Moller and M. S. Plesset. Note on an Approximation. *Physical Review*, 46(1):618–622, 1934.

[11] Martin Head-gordon and John A Pople. MP2 ENERGY EVALUATION BY DIRECT METHODS. *Chemical Physics Letters*, 153(6):503–506, 1988.

[12] Michael J Frisch, Martin Head-gordon, and John A Pople. SEMI-DIRECT ALGORITHMS FOR THE MP2 ENERGY AND GRADIENT Michael J. FRISCH. *Chemical Physics Letters*, 166(3):281–289, 1990.

[13] Michael J Frisch, Martin Head-gordon, and John A Pople. A DIRECT MP2 GRADIENT METHOD Michael J. FRISCH. *Chemical Physics Letters*, 166(3):275–280, 1990.

[14] Yan Zhao and Donald G Truhlar. The M06 suite of density functionals for main group thermochemistry , thermochemical kinetics , noncovalent interactions , excited states , and transition elements : two new functionals and systematic testing of four M06-class functionals and 12 other fun. *Theoretical Chemistry Accounts*, 120(1-3):215–241, 2007.

[15] Vincenzo Barone, Maurizio Cossi, Dipartimento Chimica, V Uni, Federico Ii, V Mezzocannone, and I Napoli. Conductor Solvent Model. *Journal of Physical Chemistry A*, 5639(97):1995–2001, 1998.

[16] Aleksandr V Marenich, Christopher J Cramer, and Donald G Truhlar. Universal Solvation Model Based on Solute Electron Density and on a Continuum Model of the Solvent Defined by the Bulk Dielectric Constant and Atomic Surface Tensions. *Journal of Physical Chemistry B*, 113:6378–6396, 2009.

[17] P N Simoes, L M Pedroso, a M Matos Beja, M Ramos Silva, Elizabeth MacLean, and a a Portugal. Crystal and molecular structure of 4,6-bis(nitroimino)-1,3,5-triazinan-2-one: theoretical and X-ray studies. *The journal of physical chemistry. A*, 111(1):150–8, 2007.

[18] Jonathan C. Rienstra-Kiracofe, Gregory S. Tschumper, Henry F. Schaefer, Sreela Nandi, and G. Barney Ellison. Atomic and molecular electron affinities: Photoelectron experiments and theoretical computations. *Chemical Reviews*, 102(1):231–282, 2002.

[19] Kristin S. Alongi and George C. Shields. Theoretical calculations of acid dissociation constants. A review article. *Annual Reports in Computational Chemistry*, 6(C):113–138, 2010.

APPENDIX

Table A1: Optimized geometry coordinates for the neutral B3LYP/6-311++G(d,p) NIC1 conformer without solvation models. All values are shown in Angstroms (Å).

Element	x	y	z
O	-3.721471	0.604082	0.086119
O	-4.423525	-1.439393	-0.095350
N	-3.540353	-0.620828	0.002323
H	-2.070708	1.485238	-0.005521
O	0.000000	2.969997	-0.051171
N	-1.170334	1.007146	-0.024801
N	-2.245898	-1.161421	0.031700
C	0.000000	1.771372	-0.034358
C	-1.220040	-0.353042	0.020397
N	1.170334	1.007146	-0.024802
N	0.000000	-0.986582	0.048094
C	1.220040	-0.353043	0.020398
H	2.070709	1.485238	-0.005516
H	0.000000	-1.999689	0.063665
N	2.245898	-1.161421	0.031701
O	3.721472	0.604080	0.086140
N	3.540353	-0.620828	0.002324
O	4.423524	-1.439392	-0.095368

Table A2: Optimized geometry coordinates for the neutral M06-2X/6-311++G(d,p) NIC1 conformer without solvation models. All values are shown in Angstroms (Å).

Element	x	y	z
O	-3.701061	0.579964	0.160793
O	-4.386474	-1.427697	-0.175192
N	-3.519394	-0.623494	0.004937
H	-2.058007	1.506304	-0.013541
O	0.000005	2.959581	-0.094040
N	-1.170150	1.010016	-0.045033
N	-2.233018	-1.157731	0.055987
C	0.000004	1.768265	-0.062614
C	-1.218988	-0.345508	0.036272
N	1.170155	1.010013	-0.045013
N	-0.000001	-0.972322	0.087135
C	1.218988	-0.345512	0.036277
H	2.058011	1.506300	-0.013494
H	-0.000003	-1.985678	0.117553
N	2.233016	-1.157738	0.055976
O	3.701061	0.579946	0.160901
N	3.519392	-0.623497	0.004936
O	4.386467	-1.427685	-0.175286

Table A3: Optimized geometry coordinates for the neutral MP2/6-311++G(d,p) NIC1 conformer without solvation models. All values are shown in Angstroms (Å).

Element	x	y	z
O	3.707730	0.585370	-0.321423
O	4.405812	-1.395569	0.256378
N	3.517709	-0.605425	-0.040323
H	2.048619	1.492332	0.023326
O	0.000046	2.960023	0.141424
N	1.168049	0.992007	0.117473
N	2.245138	-1.167823	-0.090195
C	0.000029	1.753162	0.118771
C	1.213191	-0.359627	-0.023668
N	-1.168013	0.992042	0.117448
N	-0.000010	-0.994714	-0.036443
C	-1.213191	-0.359587	-0.023739
H	-2.048566	1.492397	0.023311
H	-0.000025	-2.006276	-0.128816
N	-2.245159	-1.167757	-0.090155
O	-3.707734	0.585462	-0.321095
N	-3.517696	-0.605321	-0.039967
O	-4.405895	-1.395687	0.255856

Table A4: Optimized geometry coordinates for the neutral B3LYP/6-311++G(d,p) NIC2 conformer without solvation models. All values are shown in Angstroms (Å).

Element	x	y	z
O	-4.455810	-0.912438	-0.074906
C	0.415408	2.185648	0.027196
O	0.773205	3.331227	0.034369
N	-0.920462	1.797755	0.036620
N	1.302660	1.105328	0.009753
C	-1.380031	0.503627	0.012314
C	0.942297	-0.207749	-0.017943
N	-3.249738	-0.900632	-0.005401
O	3.614915	-0.036907	-0.155736
N	3.080440	-1.147391	-0.011948
O	3.681580	-2.184938	0.130717
N	-2.680479	0.381295	0.019858
N	-0.415789	-0.459002	-0.024890
N	1.681348	-1.282356	-0.026839
H	-1.616872	2.532873	0.052553
O	-2.538031	-1.916271	0.051076
H	-0.745893	-1.425121	-0.010804
H	2.303984	1.292736	-0.035384

Table A5: Optimized geometry coordinates for the neutral M06-2X/6-311++G(d,p) NIC2 conformer without solvation models. All values are shown in Angstroms (Å).

Element	x	y	z
O	-4.412635	-0.926771	0.176763
C	0.405525	2.179618	0.017825
O	0.757601	3.319649	0.025307
N	-0.922904	1.786604	-0.003363
N	1.299886	1.107970	0.031797
C	-1.376925	0.494050	-0.013813
C	0.946999	-0.202603	-0.002961
N	-3.231304	-0.900190	-0.010860
O	3.591874	-0.048288	-0.166524
N	3.066702	-1.142892	0.010209
O	3.660513	-2.165453	0.189027
N	-2.671093	0.375898	-0.005691
N	-0.408611	-0.460954	-0.013238
N	1.677185	-1.275252	-0.008679
H	-1.623576	2.518372	0.006629
O	-2.532559	-1.888001	-0.215794
H	-0.711256	-1.432162	-0.069710
H	2.293868	1.320025	-0.014688

Table A6: Optimized geometry coordinates for the neutral MP2/6-311++G(d,p) NIC2 conformer without solvation models. All values are shown in Angstroms (Å).

Element	x	y	z
O	-4.394850	-0.939656	0.312363
C	0.434925	2.169819	0.042059
O	0.813108	3.312843	-0.033562
N	-0.901376	1.799381	0.117222
N	1.310640	1.079098	0.113699
C	-1.381940	0.512351	0.021726
C	0.931386	-0.232004	0.032117
N	-3.235108	-0.884924	-0.059559
O	3.567552	-0.119226	-0.471323
N	3.060486	-1.144694	-0.004370
O	3.670975	-2.096741	0.449703
N	-2.682183	0.413130	-0.033654
N	-0.431790	-0.467400	0.073330
N	1.656127	-1.313131	-0.020567
H	-1.586861	2.543407	0.046018
O	-2.569327	-1.840761	-0.475424
H	-0.748036	-1.419293	-0.103719
H	2.291443	1.272999	-0.074477

Table A7: Optimized geometry coordinates for the neutral B3LYP/6-311++G(d,p) NIC3 conformer without solvation models. All values are shown in Angstroms (Å).

Element	x	y	z
O	-1.635560	-2.141854	0.234832
O	-3.713006	-1.752402	-0.253677
N	-2.584594	-1.391010	-0.014501
O	0.000000	3.851142	0.005512
N	-1.157521	1.878659	0.013762
N	-2.414258	0.007467	-0.007249
C	0.000000	2.649295	0.011509
C	-1.211303	0.505223	0.010927
N	1.157521	1.878659	0.013765
N	0.000000	-0.139157	0.009451
C	1.211303	0.505223	0.010928
H	2.041845	2.371856	0.000124
H	0.000000	-1.160733	0.102661
N	2.414258	0.007467	-0.007247
O	1.635559	-2.141854	0.234830
N	2.584594	-1.391010	-0.014501
O	3.713006	-1.752402	-0.253678
H	-2.041845	2.371856	0.000120

Table A8: Optimized geometry coordinates for the neutral M06-2X/6-311++G(d,p) NIC3 conformer without solvation models. All values are shown in Angstroms (Å).

Element	x	y	z
O	-1.626539	-2.112180	0.309528
O	-3.646897	-1.762062	-0.333186
N	-2.555650	-1.386102	-0.016926
O	0.000014	3.834652	0.005949
N	-1.154557	1.871471	0.016150
N	-2.403621	0.004664	-0.006840
C	0.000011	2.640070	0.013291
C	-1.207529	0.502606	0.013608
N	1.154576	1.871465	0.016189
N	0.000004	-0.141649	0.008970
C	1.207541	0.502600	0.013634
H	2.039435	2.364484	0.000176
H	-0.000004	-1.158339	0.130698
N	2.403628	0.004649	-0.006808
O	1.626543	-2.112181	0.309626
N	2.555635	-1.386121	-0.016916
O	3.646847	-1.762097	-0.333281
H	-2.039414	2.364493	0.000120

Table A9: Optimized geometry coordinates for the neutral MP2/6-311++G(d,p) NIC3 conformer without solvation models. All values are shown in Angstroms (Å).

Element	x	y	z
O	-1.622827	-2.135848	-0.425209
O	-3.593724	-1.758562	0.439046
N	-2.529247	-1.396580	-0.031731
O	-0.003887	3.855554	0.006342
N	-1.126895	1.874780	-0.271075
N	-2.405527	0.008860	-0.161371
C	-0.001902	2.647932	0.000978
C	-1.202584	0.505983	-0.138048
N	1.125873	1.876283	0.263940
N	0.001941	-0.140861	-0.010292
C	1.204098	0.507662	0.132946
H	2.007686	2.373007	0.327739
H	0.001150	-1.160921	-0.003092
N	2.406910	0.011223	0.165715
O	1.626284	-2.133178	0.434319
N	2.530172	-1.394406	0.034587
O	3.591835	-1.756246	-0.442538
H	-2.010549	2.369610	-0.324005

Table A10: Optimized geometry coordinates for the neutral CPCM B3LYP/6-311++G(d,p) NIC1 conformer. All values are shown in Angstroms (Å).

Element	x	y	z
O	-3.727845	0.597480	-0.059688
O	-4.416571	-1.453014	0.050181
N	-3.521812	-0.624943	-0.000765
H	-2.064910	1.493445	-0.014134
O	0.000000	2.974275	-0.000004
N	-1.167989	1.011135	-0.000193
N	-2.246705	-1.154201	0.003942
C	0.000000	1.771765	-0.000002
C	-1.211397	-0.342950	-0.000720
N	1.167989	1.011134	0.000190
N	0.000000	-0.980152	-0.000001
C	1.211397	-0.342950	0.000719
H	2.064910	1.493445	0.014134
H	0.000000	-1.994538	0.000000
N	2.246705	-1.154202	-0.003943
O	3.727844	0.597480	0.059702
N	3.521812	-0.624943	0.000767
O	4.416571	-1.453013	-0.050187

Table A11: Optimized geometry coordinates for the neutral CPCM M06-2X/6-311++G(d,p) NIC1 conformer. All values are shown in Angstroms (Å).

Element	x	y	z
O	-3.708616	0.575482	0.125054
O	-4.385075	-1.445887	-0.110027
N	-3.504854	-0.628395	0.008974
H	-2.053828	1.514865	-0.014370
O	-0.000009	2.965504	-0.074412
N	-1.168063	1.015573	-0.028491
N	-2.233464	-1.151157	0.025809
C	-0.000006	1.770600	-0.046522
C	-1.210705	-0.334508	0.017350
N	1.168056	1.015578	-0.028506
N	0.000002	-0.965798	0.043178
C	1.210706	-0.334500	0.017349
H	2.053822	1.514871	-0.014436
H	0.000006	-1.980753	0.064574
N	2.233467	-1.151147	0.025841
O	3.708620	0.575514	0.124777
N	3.504858	-0.628390	0.008974
O	4.385082	-1.445911	-0.109801

Table A12: Optimized geometry coordinates for the neutral CPCM MP2/6-311++G(d,p) NIC1 conformer. All values are shown in Angstroms (Å).

Element	x	y	z
O	3.707730	0.585370	-0.321423
O	4.405812	-1.395569	0.256378
N	3.517709	-0.605425	-0.040323
H	2.048619	1.492332	0.023326
O	0.000046	2.960023	0.141424
N	1.168049	0.992007	0.117473
N	2.245138	-1.167823	-0.090195
C	0.000029	1.753162	0.118771
C	1.213191	-0.359627	-0.023668
N	-1.168013	0.992042	0.117448
N	-0.000010	-0.994714	-0.036443
C	-1.213191	-0.359587	-0.023739
H	-2.048566	1.492397	0.023311
H	-0.000025	-2.006276	-0.128816
N	-2.245159	-1.167757	-0.090155
O	-3.707734	0.585462	-0.321095
N	-3.517696	-0.605321	-0.039967
O	-4.405895	-1.395687	0.255856

Table A13: Optimized geometry coordinates for the neutral the neutral CPCM B3LYP/6-311++G(d,p) NIC2 conformer. All values are shown in Angstroms (Å).

Element	x	y	z
O	-4.451167	-0.922238	0.000157
C	0.402202	2.186005	-0.000052
O	0.759673	3.335099	-0.000060
N	-0.928947	1.796104	-0.000107
N	1.296809	1.113473	0.000018
C	-1.371597	0.505032	-0.000052
C	0.941293	-0.191851	0.000025
N	-3.231365	-0.899032	0.000027
O	3.623685	-0.034853	0.000358
N	3.066395	-1.142893	0.000025
O	3.674917	-2.199960	-0.000276
N	-2.679517	0.366051	-0.000042
N	-0.408622	-0.453303	-0.000004
N	1.689298	-1.272066	0.000013
H	-1.628465	2.530386	-0.000119
O	-2.531744	-1.925098	-0.000052
H	-0.729458	-1.421315	-0.000015
H	2.295274	1.313867	0.000095

Table A14: Optimized geometry coordinates for the neutral CPCM M06-2X/6-311++G(d,p) NIC2 conformer. All values are shown in Angstroms (Å).

Element	x	y	z
O	-4.425477	-0.922941	0.021750
C	0.393153	2.178913	-0.019301
O	0.743918	3.322668	-0.027190
N	-0.930614	1.782785	-0.022884
N	1.295319	1.115511	-0.004949
C	-1.367304	0.493321	-0.006929
C	0.947425	-0.187573	0.008666
N	-3.218584	-0.899009	0.006666
O	3.601445	-0.044710	0.127862
N	3.057664	-1.136435	0.006386
O	3.660550	-2.175547	-0.108045
N	-2.669799	0.360393	-0.009274
N	-0.400599	-0.456275	0.011267
N	1.686556	-1.265594	0.007855
H	-1.634757	2.513558	-0.032781
O	-2.522225	-1.909699	0.003094
H	-0.696526	-1.430282	0.013481
H	2.286346	1.340959	0.019452

Table A15: Optimized geometry coordinates for the neutral CPCM MP2/6-311++G(d,p) NIC2 conformer. All values are shown in Angstroms (Å).

Element	x	y	z
O	-4.413060	-0.943421	0.242587
C	0.412750	2.178605	0.028738
O	0.782418	3.327782	-0.022554
N	-0.917364	1.796768	0.080873
N	1.300958	1.099856	0.080417
C	-1.374126	0.508195	0.014978
C	0.936931	-0.206057	0.025022
N	-3.223123	-0.893967	-0.045115
O	3.589882	-0.081614	-0.348887
N	3.057676	-1.142322	0.000604
O	3.670647	-2.150494	0.328596
N	-2.681305	0.387582	-0.014862
N	-0.418097	-0.457956	0.054030
N	1.670343	-1.291979	0.001768
H	-1.611911	2.535616	0.026545
O	-2.545836	-1.876409	-0.378045
H	-0.725894	-1.420416	-0.070444
H	2.288468	1.307728	-0.046098

Table A16: Optimized geometry coordinates for the neutral CPCM B3LYP/6-311++G(d,p) NIC3 conformer. All values are shown in Angstroms (Å).

Element	x	y	z
O	-1.616290	-2.154843	0.000495
O	-3.742226	-1.743213	-0.000521
N	-2.578877	-1.374903	-0.000047
O	0.000018	3.844595	0.000091
N	-1.159000	1.874208	-0.000036
N	-2.413134	-0.001761	-0.000077
C	0.000016	2.640120	0.000040
C	-1.204478	0.511845	-0.000027
N	1.159026	1.874202	0.000031
N	0.000006	-0.131777	0.000009
C	1.204492	0.511839	0.000023
H	2.043052	2.371071	0.000091
H	-0.000005	-1.155261	0.000211
N	2.413143	-0.001782	-0.000028
O	1.616252	-2.154843	0.000722
N	2.578860	-1.374929	-0.000028
O	3.742199	-1.743264	-0.000695
H	-2.043021	2.371086	-0.000010

Table A17: Optimized geometry coordinates for the neutral CPCM M06-2X/6-311++G(d,p) NIC3 conformer. All values are shown in Angstroms (Å).

Element	x	y	z
O	-1.599702	-2.133462	0.001837
O	-3.707508	-1.744703	-0.001714
N	-2.560102	-1.370817	-0.000045
O	0.000211	3.828020	0.000285
N	-1.156101	1.866853	-0.000035
N	-2.404319	-0.002537	-0.000091
C	0.000159	2.630834	0.000129
C	-1.200944	0.508881	-0.000008
N	1.156354	1.866754	0.000068
N	0.000035	-0.133852	-0.000204
C	1.201059	0.508784	-0.000065
H	2.041349	2.363417	0.000047
H	0.000007	-1.155439	0.000230
N	2.404378	-0.002771	-0.000207
O	1.599359	-2.133517	0.001529
N	2.559918	-1.371055	-0.000111
O	3.707254	-1.745163	-0.001484
H	-2.041049	2.363600	0.000129

Table A18: Optimized geometry coordinates for the neutral CPCM MP2/6-311++G(d,p) NIC3 conformer. All values are shown in Angstroms (Å).

Element	x	y	z
O	-1.590943	-2.141625	-0.334892
O	-3.640961	-1.788954	0.310559
N	-2.529799	-1.397554	-0.024574
O	-0.027609	3.852913	0.078558
N	-1.159066	1.874664	-0.156473
N	-2.407668	-0.008826	-0.077470
C	-0.015108	2.645455	0.010534
C	-1.204212	0.510123	-0.095283
N	1.146444	1.886356	0.051674
N	0.005105	-0.127101	-0.073458
C	1.203168	0.522063	0.041455
H	2.023884	2.387682	0.150619
H	0.008222	-1.146046	-0.027538
N	2.409634	0.012065	0.095547
O	1.597509	-2.125749	0.328311
N	2.542926	-1.376158	0.052638
O	3.669414	-1.761167	-0.235046
H	-2.047497	2.365037	-0.118419

Table A19: Optimized geometry coordinates for the neutral SMD B3LYP/6-311++G(d,p) NIC1 conformer. All values are shown in Angstroms (Å).

Element	x	y	z
O	3.731762	0.592555	-0.050647
O	4.411352	-1.462058	0.036681
N	3.512395	-0.628024	-0.005330
H	2.059425	1.509978	0.006443
O	0.000007	2.976139	0.026563
N	1.167599	1.015099	0.014167
N	2.245208	-1.150629	-0.006157
C	0.000005	1.769045	0.018761
C	1.206659	-0.335636	-0.003729
N	-1.167592	1.015104	0.014172
N	-0.000001	-0.974601	-0.012559
C	-1.206659	-0.335632	-0.003731
H	-2.059416	1.509987	0.006448
H	-0.000003	-1.991835	-0.019495
N	-2.245209	-1.150622	-0.006142
O	-3.731772	0.592557	-0.050638
N	-3.512399	-0.628019	-0.005288
O	-4.411353	-1.462061	0.036636

Table A20: Optimized geometry coordinates for the neutral SMD M06-2X/6-311++G(d,p) NIC1 conformer. All values are shown in Angstroms (Å).

Element	x	y	z
O	3.709290	0.572065	-0.131373
O	4.380827	-1.447337	0.129017
N	3.495439	-0.628929	-0.006775
H	2.049023	1.527489	0.022550
O	0.000110	2.964075	0.078166
N	1.167697	1.016150	0.032921
N	2.232816	-1.149281	-0.031752
C	0.000072	1.764721	0.049191
C	1.205784	-0.330162	-0.026184
N	-1.167601	1.016223	0.032915
N	-0.000017	-0.963110	-0.063934
C	-1.205779	-0.330089	-0.026178
H	-2.048893	1.527619	0.022565
H	-0.000047	-1.981168	-0.087767
N	-2.232844	-1.149176	-0.031736
O	-3.709455	0.572085	-0.131406
N	-3.495497	-0.628886	-0.006760
O	-4.380833	-1.447350	0.129035

Table A21: Optimized geometry coordinates for the neutral SMD MP2/6-311++G(d,p) NIC1 conformer. All values are shown in Angstroms (Å).

Element	x	y	z
O	3.716119	0.586123	-0.254133
O	4.396958	-1.417681	0.254728
N	3.509598	-0.612342	-0.019490
H	2.047038	1.508731	0.027119
O	0.000048	2.963089	0.117571
N	1.167820	0.998465	0.099764
N	2.242605	-1.163075	-0.093070
C	0.000033	1.752834	0.096314
C	1.209049	-0.348621	-0.045828
N	-1.167774	0.998495	0.099783
N	-0.000007	-0.982293	-0.097476
C	-1.209044	-0.348589	-0.045813
H	-2.046981	1.508783	0.027159
H	-0.000020	-1.998253	-0.170797
N	-2.242616	-1.163031	-0.093089
O	-3.716210	0.586120	-0.254192
N	-3.509633	-0.612341	-0.019571
O	-4.396943	-1.417669	0.254842

Table A22: Optimized geometry coordinates for the neutral SMD B3LYP/6-311++G(d,p) NIC2 conformer. All values are shown in Angstroms (Å).

Element	x	y	z
O	-4.452245	-0.921719	-0.000627
C	0.393094	2.178838	-0.000359
O	0.748372	3.333965	-0.001155
N	-0.933062	1.790808	0.000753
N	1.294706	1.116897	0.000056
C	-1.365739	0.500870	0.000760
C	0.942161	-0.185654	0.000630
N	-3.225599	-0.896948	-0.000294
O	3.628233	-0.033139	0.000177
N	3.063545	-1.136770	-0.000113
O	3.678219	-2.197883	-0.000845
N	-2.678335	0.358730	0.000504
N	-0.404192	-0.455379	0.001428
N	1.695954	-1.266985	0.000452
H	-1.631823	2.529559	-0.000548
O	-2.534195	-1.927956	-0.000824
H	-0.714203	-1.428387	0.001284
H	2.290739	1.335884	-0.000242

Table A23: Optimized geometry coordinates for the neutral SMD M06-2X/6-311++G(d,p) NIC2 conformer. All values are shown in Angstroms (Å).

Element	x	y	z
O	-4.427029	-0.922236	-0.000446
C	0.384571	2.171497	-0.000435
O	0.733588	3.321126	-0.001877
N	-0.934656	1.777901	0.001090
N	1.293006	1.118092	0.000108
C	-1.361640	0.489391	0.000991
C	0.947434	-0.181786	0.000849
N	-3.213753	-0.896788	-0.000461
O	3.607043	-0.036284	0.000668
N	3.055349	-1.130375	-0.000096
O	3.664978	-2.178996	-0.001476
N	-2.669038	0.353921	0.000637
N	-0.396819	-0.458792	0.002012
N	1.693190	-1.261112	0.000738
H	-1.638079	2.513781	-0.000841
O	-2.525419	-1.912293	-0.001526
H	-0.683288	-1.437800	0.001853
H	2.282929	1.358939	-0.000377

Table A24: Optimized geometry coordinates for the neutral SMD MP2/6-311++G(d,p) NIC2 conformer. All values are shown in Angstroms (Å).

Element	x	y	z
O	-4.404667	-0.954969	0.249267
C	0.407304	2.170791	0.024526
O	0.776927	3.323621	-0.034889
N	-0.919694	1.794952	0.083651
N	1.299194	1.100226	0.074083
C	-1.370173	0.508021	0.025681
C	0.933773	-0.201750	0.039317
N	-3.215219	-0.891176	-0.052823
O	3.583647	-0.079351	-0.353582
N	3.050778	-1.138719	0.000415
O	3.674766	-2.149214	0.313811
N	-2.680791	0.384784	-0.005319
N	-0.417588	-0.458043	0.080740
N	1.671833	-1.289239	0.027483
H	-1.610470	2.540184	0.017876
O	-2.543462	-1.866783	-0.415247
H	-0.718911	-1.425810	-0.034586
H	2.286690	1.317330	-0.052921

Table A25: Optimized geometry coordinates for the neutral SMD B3LYP/6-311++G(d,p) NIC3 conformer. All values are shown in Angstroms (Å).

Element	x	y	z
O	-1.619931	-2.154671	-0.000146
O	-3.745353	-1.739246	0.000342
N	-2.576681	-1.366502	0.000019
O	-0.000061	3.838693	0.000389
N	-1.158822	1.870518	-0.000188
N	-2.412401	-0.003473	-0.000170
C	-0.000035	2.629250	0.000076
C	-1.199951	0.512727	-0.000236
N	1.158758	1.870554	-0.000087
N	-0.000004	-0.133712	-0.000361
C	1.199947	0.512748	-0.000160
H	2.042716	2.374464	0.000577
H	-0.000046	-1.157762	-0.000322
N	2.412395	-0.003389	-0.000190
O	1.620010	-2.154651	0.000430
N	2.576724	-1.366480	0.000084
O	3.745407	-1.739136	-0.000022
H	-2.042790	2.374410	-0.000033

Table A26: Optimized geometry coordinates for the neutral SMD M06-2X/6-311++G(d,p) NIC3 conformer. All values are shown in Angstroms (Å).

Element	x	y	z
O	-1.604265	-2.126812	0.155822
O	-3.692312	-1.750908	-0.145982
N	-2.551687	-1.364550	-0.005942
O	-0.000069	3.823520	0.022061
N	-1.156406	1.864818	0.007495
N	-2.402854	-0.004576	-0.018559
C	-0.000052	2.621363	0.012595
C	-1.196840	0.511371	-0.005482
N	1.156312	1.864859	0.006975
N	-0.000010	-0.133523	-0.020391
C	1.196865	0.511386	-0.005586
H	2.041265	2.369226	0.013602
H	-0.000001	-1.154877	0.016355
N	2.402862	-0.004454	-0.018593
O	1.604256	-2.126832	0.155044
N	2.551733	-1.364567	-0.005982
O	3.692470	-1.750747	-0.145421
H	-2.041397	2.369126	0.013666

Table A27: Optimized geometry coordinates for the neutral SMD MP2/6-311++G(d,p) NIC3 conformer. All values are shown in Angstroms (Å).

Element	x	y	z
O	-1.575453	-2.148649	-0.296582
O	-3.636843	-1.790652	0.302140
N	-2.519563	-1.396160	-0.021415
O	-0.039775	3.845415	0.083233
N	-1.159388	1.868943	-0.195242
N	-2.403515	-0.015765	-0.095428
C	-0.022773	2.634115	0.013092
C	-1.198361	0.508465	-0.115159
N	1.138135	1.885746	0.102310
N	0.007767	-0.128003	-0.082045
C	1.199161	0.526362	0.052749
H	2.012302	2.397569	0.207403
H	0.008457	-1.148316	-0.039129
N	2.409447	0.017567	0.094499
O	1.608452	-2.114839	0.366178
N	2.538820	-1.363391	0.047493
O	3.653495	-1.754824	-0.287576
H	-2.049843	2.362926	-0.162709